euspen's 22nd International Conference & Exhibition, Geneva, CH, May/June 2022
www.euspen.eu

Thermal error compensation of machine tools based on thermal mode shapes – a modelling case study

Beñat Iñigo[1], Natalia Colinas-Armijo[1], Gorka Aguirre[1], Luis Norberto López de Lacalle[2], Harkaitz Urreta[1]

[1]*IDEKO member of Basque Research and Technology Alliance, Elgoibar (Basque Country), Spain*
[2]*Euskal Herriko Unibertsitatea (EHU-UPV) Dept. Mechanical Engineering, Bilbao (Basque Country), Spain*

binigo@ideko.es

Abstract

Thermal errors represent one of the main error sources regarding the volumetric accuracy of machine tools. Real time thermal error compensation comes as a relatively low-cost solution to improve the accuracy of machine tools. The estimation is usually based on temperatures measured on certain points in the machine and a compensation model that is obtained from some training tests where temperatures and thermal errors are measured. After the initial test is done, the model is usually verified by periodic measurements throughout the machine working life, but such measurements should be kept to a minimum, as they affect the productivity of the machine. In this work, a thermal monitoring system is presented based on the Proper Orthogonal Decomposition reduction of an initial thermal test. This surveillance system proved to be useful to detect erratic thermal behavior or the apparition of new uncharacterized heat sources. An adaptive compensation approach was presented capable of adapting its inputs according to the temperature behavior.

Keywords: Thermal error compensation, Optimal sensor position; Proper Orthogonal Decomposition, Adaptive Model, Machine Tool

1. Introduction

Thermal errors are one of the main contributors to the volumetric error of machine tools, causing relative displacement between workpiece and Tool Center Point (TCP). Numerical compensation relies on model-based prediction of the thermoelastic deformation of the machine and it is a relatively low-cost solution to improve the accuracy of machine tools once they are placed on the shopfloor.

Extensive research has been done on developing effective compensation models [1]. They are usually based on temperature measurements and other available machine data to obtain reliable models that can predict the thermal behavior in real time. Ideally, this compensation models should be able to capture and compensate different error sources such as localized heat sources (e.g. main spindle bearings), environmental or distributed effects (varying ambient) or even moving heat sources (ball screw, conduction through moving parts).

An initial training phase, measuring TCP displacements, is usually carried out in order to obtain the compensation model, where the correlation between temperature sensors and displacements is identified [2]. Alternatively, structure-based compensation models, physical representations of the thermoelastic functional chain, can be designed, optimized and trained in a virtual environment [3], saving machine occupation time. Even so, their performance needs to be validated in a real working environment in order to consider modelling errors or uncertainties.

Due to the necessity to minimize machine occupation time, the compensation model has to be able to predict thermal behavior beyond training phase with none or limited displacement measurements. Yet, developing such a robust model would need long training tests and excitation of all possible heat sources, which is not always possible. Furthermore, conditions in or around the machine tool can change. These changes should be detected so that the model can be retrained. Several works have been focused on adaptive models and varying measuring frequencies to overcome this problem [4].

When large amount of temperature data is available (either from simulation or actual on-machine measurements) reduction techniques, such as Proper Orthogonal Decomposition (POD) based approaches, allow to identify dominant trends in the thermal field. They are usually combined with optimal sensor placement procedures in order to select the optimal location and number of sensors needed to compensate certain thermal behaviors [5].

In [6], a thermal error compensation solution for local and distributed thermal effects was proposed, based on POD and stablished optimal sensor placement procedures. The model showed good prediction capability, even when the amplitude and frequency of the characterized heat sources changed. In this work a modification of this approach is presented, capable of monitoring the thermal state of the machine and detect temperature behaviors that differ from those of the training phase. Furthermore, an adaptive compensation model is developed, that changes according to these outliers detected in the temperature data. In section 2, basics of POD and optimal sensor placement, as well as the compensation model are explained. In section 3, a FE model of a machine column with different load cases is presented. In section 4, thermal monitoring and adaptive compensation are implemented in a virtual environment to show the functioning of the approach. Section 5 closes with conclusions.

2. Compensation model based on POD

2.1. POD based reduction and optimal sensor placement

Proper Orthogonal Decomposition is a Model Order Reduction (MOR) technique that uses Singular Value Decomposition (SVD) to capture and classify the dominant modes of any data set stored in a matrix. Applied to thermomechanical systems, POD is used to reduce the temperature field so that it can be

represented with orthogonal thermal modes that describe its spatial and temporal evolution.

The temperature field is arranged in the so-called snapshot matrix of dimension nxm, with the rows representing n different nodes or temperature sensors and the columns m time instants. By selecting the first r dominant modes (with $r \ll n$) a reduced modal basis Φ_r, of dimension nxr, can be obtained capturing almost all the information with just a few dominant modes.

$$\boldsymbol{T}(t) \approx \boldsymbol{\Phi}_r \cdot \hat{\boldsymbol{T}}(t) \tag{1}$$

where T represents the full thermal field and $\hat{T}$ the coefficients multiplying each mode at a given instant. In order to implement a compensation model, the coefficients in $\hat{\boldsymbol{T}}$ need to be estimated in real time from actual temperature measurements.

Optimal sensor placement strategies have been widely used in order to select the optimal measurement points to estimate coefficients in $\hat{\boldsymbol{T}}$. In this work, a similar approach to the one described in [5] is used, where the sensors are selected in a sequential way based on covariance matrix between measurements. In order to estimate the state of r thermal modes, a minimum of $s = r$ sensors will be needed.

In order to estimate $\hat{\boldsymbol{T}}$, system in eq. (1) is solved by means of least squares (see eq. (2) and (3)). but selecting only the rows corresponding to the sensor selection.

$$\boldsymbol{T}_s \approx \boldsymbol{\Phi}_r(n_s) \cdot \hat{\boldsymbol{T}} \tag{2}$$

$$\hat{\boldsymbol{T}}(t) \approx \mathbf{A} \cdot \boldsymbol{T}_s(t) \quad \text{where} \quad \boldsymbol{A} = \boldsymbol{\Phi}_r{}^{+}(n_s) \tag{3}$$

where n_s is the subset of selected nodes to be measured, $\boldsymbol{T}_s(t)$ represents the temperature measurements in the n_s spots (with $s \geq r$) and $\mathbf{A}$ is the pseudoinverse of $\boldsymbol{\Phi}_r(n_s)$, i.e. the relation between sensors and thermal mode coefficients. Combining equations (1) and (3), the full thermal field can be approximated from the measurement of just a few sensors.

Details on the sensor selection procedure can be found in [5]. Once the temperature field has been estimated, the thermoelastic coupling matrix of the FE model is used to compensate displacement at any given point or points.

2.2. Temperature monitoring

According to the previous section the real time temperature predictor is constructed as follows:

$$\mathbf{T}(t)_{nx1} \approx \boldsymbol{\Phi}_{r_{nxr}} \cdot \mathbf{A}_{rxs} \cdot \boldsymbol{T}_s(t)_{sx1} = \boldsymbol{M} \cdot \boldsymbol{T}_s(t)_{sx1} \tag{4}$$

where M represents the temperature prediction model that relates measured temperatures with the full temperature field, that will depend on the selected r modes and n_s temperatures. This means that the measured temperatures $\boldsymbol{T}_s$ are also self-predicted in $\boldsymbol{T}$.

If the number of sensors equals the number of modes a trivial solution is achieved in $\boldsymbol{M}$ for the n_s temperatures, with unitary coefficients in the corresponding columns. This means that each node is just predicting its own value through direct output and is independent from the other temperatures in $\boldsymbol{T}_s$.

$$s = r \quad \Rightarrow \quad \mathbf{T}_{n_s} = \mathbf{T}_s \tag{5}$$

If the selected number of nodes is bigger than the number of modes an overdetermined system is obtained in eq (3). When recombining with eq. (4) the temperature predictions of the n_s nodes are no longer independent. This means that the self-prediction of the n_s temperatures will not be exact, and will only hold if the thermal behavior of the machine going on is similar to the interval where the original temperature matrix was recorded.

$$s > r \quad \Rightarrow \quad \mathbf{T}_{n_s} \approx \mathbf{T}_s \tag{6}$$

$$\boldsymbol{E}_s = \mathbf{T}_s - \mathbf{T}_{n_s} \tag{7}$$

The error term in eq. (7) represents the self-predicting errors of the model at measured temperatures. Therefore, the temperature behavior of the machine can be monitored by measuring $\boldsymbol{T}_s$ and computing eq. (4) in real time. Errors in $\boldsymbol{E}_s$ will indicate whether the thermal behavior is similar to the model training phase or not. If $\boldsymbol{E}_s$ increases, it would indicate that there is some thermal phenomena that was not adequately captured in the training test.

2.3. Adaptive thermal model

Furthermore, outlier temperatures (i.e. the ones that are not behaving as expected), can be detected from eq. (7) by selecting the ones with the highest deviations. Nodes with self-predicting errors over certain tolerance are eliminated from n_s and the model is recalculated from equations (3) and (4). This will always be possible as long as the number of nodes in n_s is still higher than r. Temperature prediction of eliminated nodes is still computed so that they can be reincorporated to the model when the error falls below the tolerance again. The functioning of this adaptive compensation system is illustrated in Figure 1.

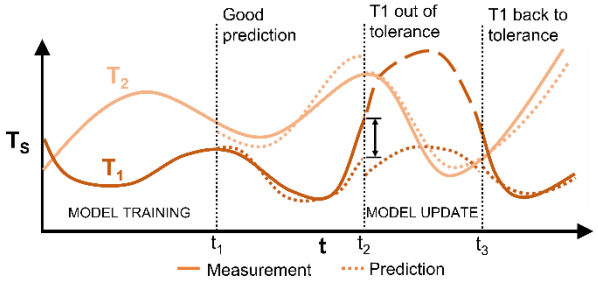

Figure 1. Illustrative example of the adaptive thermal model. At t_1 model starts predicting, after training is done. At t_2, T1 gets out of tolerance, so the model is updated ignoring it. At t_3, it is incorporated again.

3. Case study

3.1. Column model

A milling machine column Finite Element (FE) model has been developed and it is used as a case study. The FE model, as well as the main heat sources affecting the column, are shown in Figure 2. A local heat source Q1 (e.g. heat generated by a motor or an auxiliary system located in this area) has been defined at a fixed location. A moving heat source Q2 (e.g. heat being conducted from the ram to the column as the vertical axis moves) is defined near the theorical location of the vertical guideways. An additional local source Q3 has been defined for validation purposes (see section 3.3) External surfaces exchange heat with the varying ambient by convection. Thermal conductivity was set at 50 W/m·ºC and the specific heat to 500 J/kg·ºC.

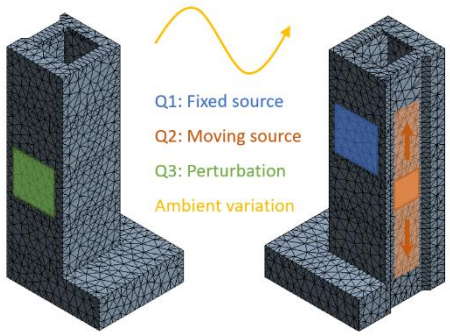

Figure 2. Finite Element model of the column and main heat sources.

3.2. Model training

In order to obtain a compensation model, the temperature of the machine has to be registered during a training test and arranged as a snapshot matrix. In this case, a transient thermoelastic simulation is carried out, where all heat sources defined in section 3.1 are varied. Step inputs in Q1 and Q2 are introduced with amplitudes of 200W and 250W respectively, as well as sinusoidal variation of ±2°C and 24h period in the ambient. Position of Q2 is also varied at two different speeds. Details of the amplitude and position variation of the heat sources are shown in Figure 3.

The temperature of each node is registered every 100 seconds and stored in the snapshot matrix T. A snapshot of the thermal field at a given instant is plotted in Figure 4, where the effects of the heat sources are clearly appreciated.

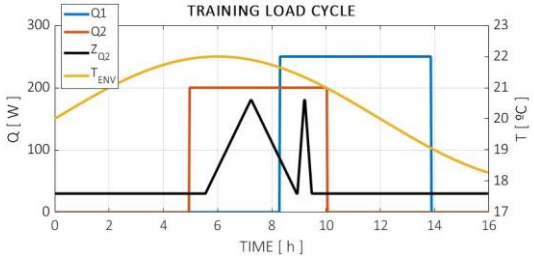

Figure 3. Training load cycle for the of the compensation model. Approximate vertical movement of Q2 (in black) is also represented.

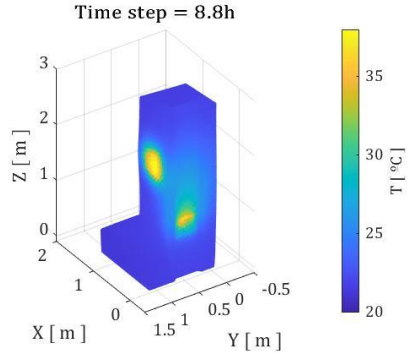

Figure 4. Snapshot of the temperature of the machine at t=8.8h

Following the procedure described in section 2, the snapshot matrix of temperatures is decomposed using SVD, and reduced by selecting the first dominant r modes. In this case, selecting $r = 15$ modes was enough to capture the 99% of the information in T. This suggests that, as long as the thermal field varies in a similar way to the testing cycle, 15 modes will be enough to predict the behavior of the full temperature field.

e

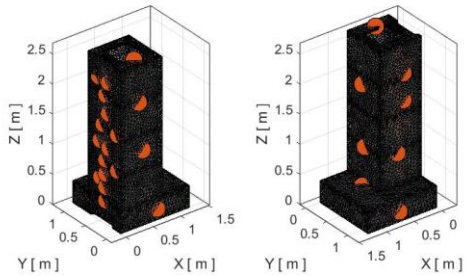

Figure 5. Front and back view of the column with the node distribution resulting of the optimal node selection with r=15 modes and s=25 nodes.

3.3. Model testing

In order to validate the compensation model a testing cycle is defined. For this purpose, load sources present in the training cycle are varied in a different way: Warm-up cycle of varying amplitudes is defined for local source Q1, trajectory in Z is changed with 3 different velocities for Q2 and ambient temperature phase and amplitude is varied. Additionally, a third heat source Q3 is introduced at the second half of the testing cycle, in order to prove the temperature monitoring ang adaptive model. Details of the amplitude and position variation of the heat sources are shown in Figure 6.

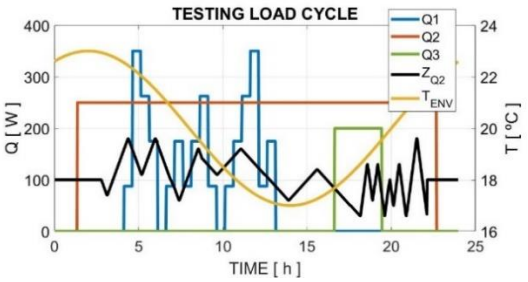

Figure 6. Testing load cycle with an extra heat source (in green).

4. Thermal monitoring and adaptive model

In this section the performance of the thermal monitoring and the adaptive compensation model are evaluated using the testing cycle defined in section 3.3.

First of all, the performance of the temperature prediction model M is evaluated by computing the Root Mean Square (RMS) error of the overall temperature field at each time step. Figure 7 shows the error throughout the testing cycle.

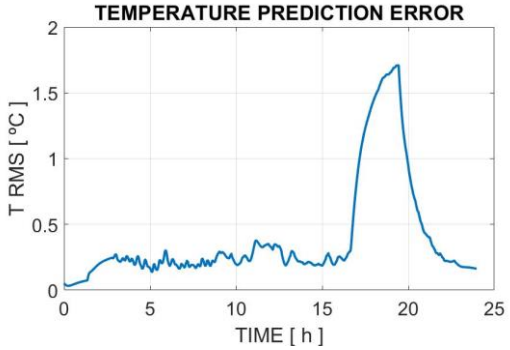

Figure 7. RMS error of the full temperature prediction throughout the testing cycle.

As it can be seen, the model predicts the temperature field with relatively good accuracy as long as thermal conditions remain similar to the training test, even if the amplitudes, frequencies and feed rates of the loads are varied (see Figure 6). However, when Q3 is turned on, the model loses accuracy as expected and it comes back when the effects of Q3 dissipate.

In real on-machine implementation the full temperature field will not be available, but only a few sensor measurements in the selected spots (n_s). However, by observing the self-prediction error $\boldsymbol{E_s}$ (see eq. (7)), disturbance introduced by Q3 can also be observed. The evolution of $\boldsymbol{E_s}$ is shown in Figure 8 for each of the sensors.

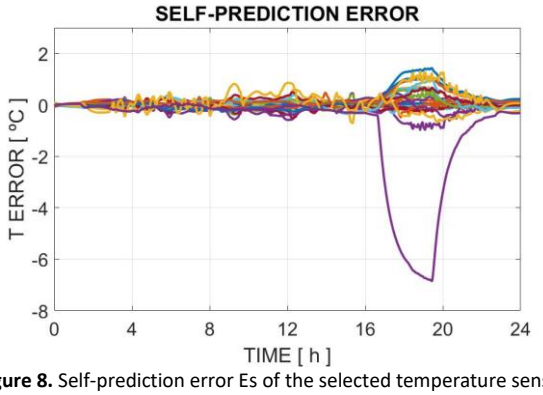

Figure 8. Self-prediction error Es of the selected temperature sensors.

As expected, sensors near the heat source Q3 show the largest deviation from its predicted value. By stablishing tolerance thresholds, a temperature surveillance system can be implemented. To avoid large data storage, prediction error is only calculated in a moving window of the las 10 time steps. To illustrate the functioning of the system Figure 9 shows the state of the temperature prediction at t=17h. Sensors out of ±0.8^{o}C tolerance are shown in red, those between ±0.4^{o}C and ±0.8^{o}C are shown in yellow and the ones inside ±0.4^{o}C in green.

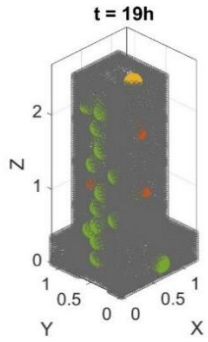

Figure 9. Temperature prediction state at t=19h

Though, predicted values are interdependent through the self-prediction model, and therefore, other sensors located further away from heat source are also affected by the values of the erratic sensors. This problem is faced by detecting and eliminating the outliers and updating the compensation model with the remaining sensors (see section 2.2). Simulation from 3.3 is carried out again, but this time allowing the adaptive modelling. Figure 10 shows the self-prediction error of the measured temperatures for adaptive compensation.

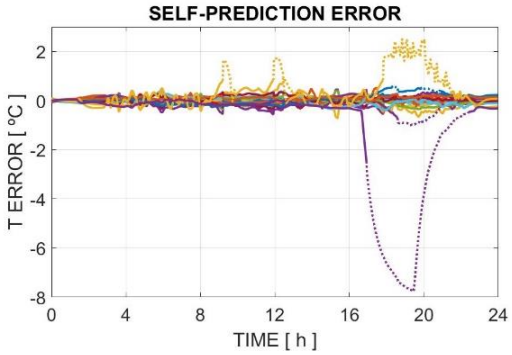

Figure 10. Self-prediction error with adapting compensation model. Nodes eliminated from the model are plotted with dot lines.

With the perturbation of Q3, the temperature near the heat source (purple outlier in Figure 10) got out of tolerance at t=17h, and therefore, was eliminated from the compensation model. A temperature near the moving source (yellow outlier in Figure 10) also showed an erratic behavior and was eliminated from the model at several points throughout the test. Comparison between Figure 8 and Figure 10 shows that several temperature predictions were being affected by the outlier temperature. Once the outlier temperatures were eliminated from the model, the remaining ones were again in accordance with the prediction inside the stablished tolerance. When Q3 was shut down, the erratic temperatures slowly returned to tolerance and were finally reincorporated to the model.

As explained in section 2.1, thermoelastic and elastic matrix of the FE model were used to obtain the compensation of every node in the column using the prediction of the temperature field. Figure 11 show trajectory prediction for several nodes located at different points of the column.

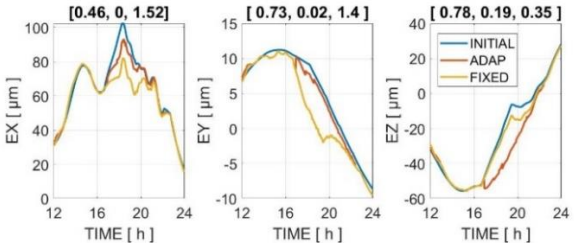

Figure 11. Trajectory prediction for 3 different points. Actual trajectory is shown against predicted by fixed (yellow) and adaptive (red) model.

Displacement prediction error was relatively good at different points of the column until disturbance Q3 was turned on. Sudden changes due to model updates can be observed at t=17h and t=19h. Prediction of the points further away from Q3 heat source (EX and EY errors in Figure 11) was improved, compare to the case were the model remains fixed. However, prediction in the nodes near the heat source was worsened. Therefore, eliminating nodes with erratic behavior from the model demonstrated to be a good decision, as it allows to compensate the effects that were characterized in the training cycle and ignore the ones that make the model malfunction.

5. Conclusions

Compensation model was presented that proves to work properly when amplitude, phase and position of the heat sources vary, as long as they had been excited in training test.

Temperature monitoring system was implemented, a surveillance system that allows to easily identify thermal behavior that differs from training phase. This allows to take corrective actions like restarting model training under new thermal conditions or checking faulty machine elements that may be causing the thermal distortion.

An adaptive compensation model was also implemented. Responding to the information of the surveillance system, nodes were eliminated or incorporated to the model in order to eliminate unknown phenomena from the prediction but still compensate expected behavior.

This work is focused on simulation results in order show the methodology. However, implementation in real machines and experimental thermal tests will be carried out in the near future.

References

[1] J. Mayr, J. Jedrzejewski, E. Uhlmann, M. Alkan Donmez, W. Knapp, F. Härtig, K. Wendt, T. Moriwaki, P. Shore, R. Schmitt, C. Brecher, T. Würz and K. Wegener, "Thermal issues in machine tools," *CIRP Annals,* vol. 61, p. 771–791, 1 2012.

[2] M. Mareš, O. Horejš and L. Havlík, "Thermal error compensation of a 5-axis machine tool using indigenous temperature sensors and CNC integrated Python code validated with a machined test piece," *Precision Engineering,* vol. 66, p. 21–30, 11 2020.

[3] S. Ihlenfeldt, S. Schroeder, L. Penter, A. Hellmich eta B. Kauschinger, «Adjustment of uncertain model parameters to improve the prediction of the thermal behavior of machine tools,» *CIRP Annals,* 1. bol.69, 5 2020.

[4] N. Zimmermann, M. Breu, J. Mayr and K. Wegener, "Autonomously triggered model updates for self-learning thermal error compensation," *CIRP Annals,* 5 2021.

[5] P. Benner, R. Herzog, N. Lang, I. Riedel eta J. Saak, «Comparison of model order reduction methods for optimal sensor placement for thermo-elastic models,» Engineering Optimization, %1. bol.51, p. 465–483, 3 2019.

[6] N. Colinas-Armijo, B. Iñigo, L. Lacalle eta G. Aguirre, «Optimal temperature sensor placement for error compensation of distributed thermal effects,» in *International Conference on Thermal Issues in Machine Tools*, 2021.